Anthropogenic Climate Change and the Record-High Temperature of May 2020 in Western Europe

Nikolaos Christidis and Peter A. Stott

The extremely warm May of 2020 in western Europe was favored by persistent high pressure, but human influence is also estimated to have made such events 40 times more likely.

Extremely warm temperature anomalies over western Europe in May 2020 (Fig. 1a) were characterized by summer-like extremes, with several French cities recording temperatures above 30°C for the first time in May, while in Spain temperatures locally exceeded 35°C. The event was linked to an omega blocking ridge pattern associated with significant warm advection over the region. Anomalies of the 500-hPa geopotential height (Z500) from the NCEP–NCAR reanalysis (Kalnay et al. 1996) illustrate the prevalent anticyclonic conditions over western Europe in May 2020 (Fig. 1b). The anticyclonic pattern was embedded in a Rossby wave train extending over the whole Northern Hemisphere (see the online supplemental material), which was also linked to the severe heatwave in Siberia (Ciavarella et al. 2021). Interestingly, the month of May also had record warmth on a global scale (Di Liberto 2020). Here we present an attribution study that assesses how anthropogenic forcings may have changed the likelihood of extreme May temperatures in western Europe (10°E–5°W, 35°–55°N), both in the general case (i.e., under any possible synoptic conditions; unconditional analysis) and under the influence of a persistent anticyclonic circulation pattern (conditional analysis).

AFFILIATIONS: Christidis and Stott—Met Office Hadley Centre, Exeter, United Kingdom

CORRESPONDING AUTHOR: nikos.christidis@metoffice.gov.uk

DOI: 10.1175/BAMS-D-21-0128.1

A supplement to this article is available online (10.1175/BAMS-D-21-0128.2)

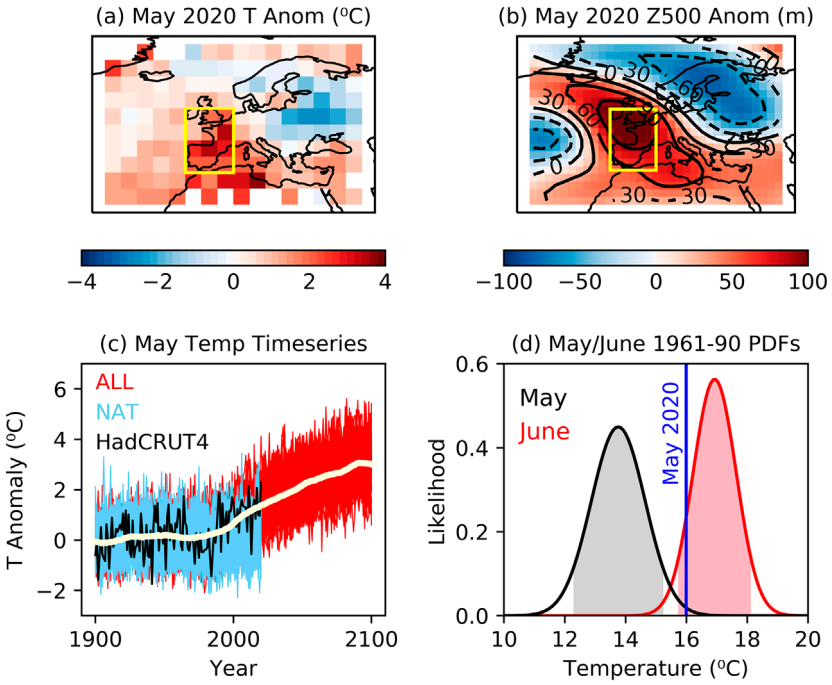

Fig. 1. Spatial patterns of the (a) temperature anomalies and (b) Z500 anomalies relative to 1961–90 for the month of May 2020 constructed with HadCRUT4 and NCEP–NCAR reanalysis data respectively. The yellow box marks the western European region considered in this study, selected as a European area that includes the warmest observed anomalies. (c) Time series of the May mean anomalies relative to 1901–30 averaged over the western European region. Time series were produced with HadCRUT4 data (black) and CMIP6 simulations with (red) and without (blue) human influence. The smoothed mean of the ALL simulations is marked by the thick white line. (d) Normal distributions of the 1961–90 actual mean temperature in western Europe for the months of May (black) and June (red) constructed with NCEP–NCAR reanalysis data. The colored areas lie between the 5th and 9th percentiles. The vertical blue line marks the May 2020 temperature.

Observed analysis and CMIP6 data.

We use the HadCRUT4 observational surface temperature dataset (Morice et al. 2012) to compute regional mean May temperature anomalies. As in other attribution studies (Bindoff et al. 2013), we define anomalies relative to a period earlier than the common 1961–90 (here we use years 1901–30 as a baseline), since the earlier baseline is closer to the pre-industrial climate and thus allows us to capture most of the anthropogenic effect. HadCRUT4 time series since 1900 are illustrated in Fig. 1c and demonstrate that May 2020 is the warmest May in the record. We also construct distributions of monthly actual temperatures over a recent period with NCEP–NCAR reanalysis data for May and June (Fig. 1d). The distributions reveal that the May 2020 temperature is extreme for the month of May, but typical for June, which could manifest a change in seasonality in a warming climate (Christidis et al. 2007; Ruosteenoja et al. 2015).

We next compute temperature anomalies with data from 11 models (see the supplemental material) that contributed to the phase 6 of the Coupled Model Intercomparison Project (CMIP6; Eyring et al. 2016). We select models that provide ensembles of simulations with all historical forcings (ALL) and natural forcings only (NAT) that enable us to compare the likelihood of extremes in the real world and in a hypothetical natural world without the effect of human activity, following the popular risk-based attribution framework (Stott et al. 2016). The ALL simulations were extended to 2100 with the "middle-of-the-road" emissions scenario SSP2–4.5 (Riahi et al. 2017). We use in total 56 ALL and 62 NAT simulations. We apply standard evaluation tests for multimodel ensembles (Christidis et al. 2021; also see the supplemental material), which show that the modeled historical trends of the regional May mean temperature are consistent with HadCRUT4, but the modeled variability is somewhat larger. We therefore bias-correct the modeled data following the approach of Christidis and Stott (2021), whereby we remove the smoothed ensemble mean from the individual ALL time series, adjust their variability, and reintroduce the ensemble mean. After bias correction the modeled variability and temperature distribution agree well with HadCRUT4 (supplemental material). We highlight the bias correction as a caveat in our analysis, which may adversely affect future likelihood estimates, if future changes in variability are incorrectly represented by the models. Nevertheless, neither the observations nor the models suggest major changes

in variability with time. Time series of the model simulations are depicted in Fig. 1c. Unlike the largely stationary NAT climate, the ALL experiment shows a steady temperature increase since the late twentieth century, leading to a warming of over 2°C by 2100 under SSP2–4.5.

Unconditional attribution.

We first compare the present-day likelihood of exceeding the 2020 observed anomaly (2.3°C) irrespective of the atmospheric circulation with what it might have been in the NAT climate. We construct the ALL distribution of May mean temperature anomalies using simulated data in years 2015–25 (56 simulations × 11 years). As the natural climate is stationary in the long run, we utilize simulated NAT anomalies of all available years. We find a major shift of the distribution toward warmer temperatures (Fig. 2a), leading to an estimated increase in the likelihood of the 2020 event of about 40-fold (Fig. 2b, Table 1). Its return time (inverse probability) is estimated to decrease from several centuries in the NAT world to about a decade in the present climate (Table 1), while by 2100 such an event could occur almost every year (estimate based on ALL data in years 2090–2100). As in previous work, extreme probabilities are calculated with the generalized Pareto distribution and associated uncertainties with a simple Monte Carlo bootstrap procedure (Christidis et al. 2013).

The available CMIP6 models contributed unequal number of simulations to our analysis, which introduces an uncertainty to our results. For example, the large number of CanESM5 simulations gives more weight to a model with a high climate sensitivity. We assess the associated uncertainty by removing the CanESM4 simulations from the ALL and NAT ensembles and repeating the analysis. We find that the ALL return time (best estimate) increases from 8.9 to

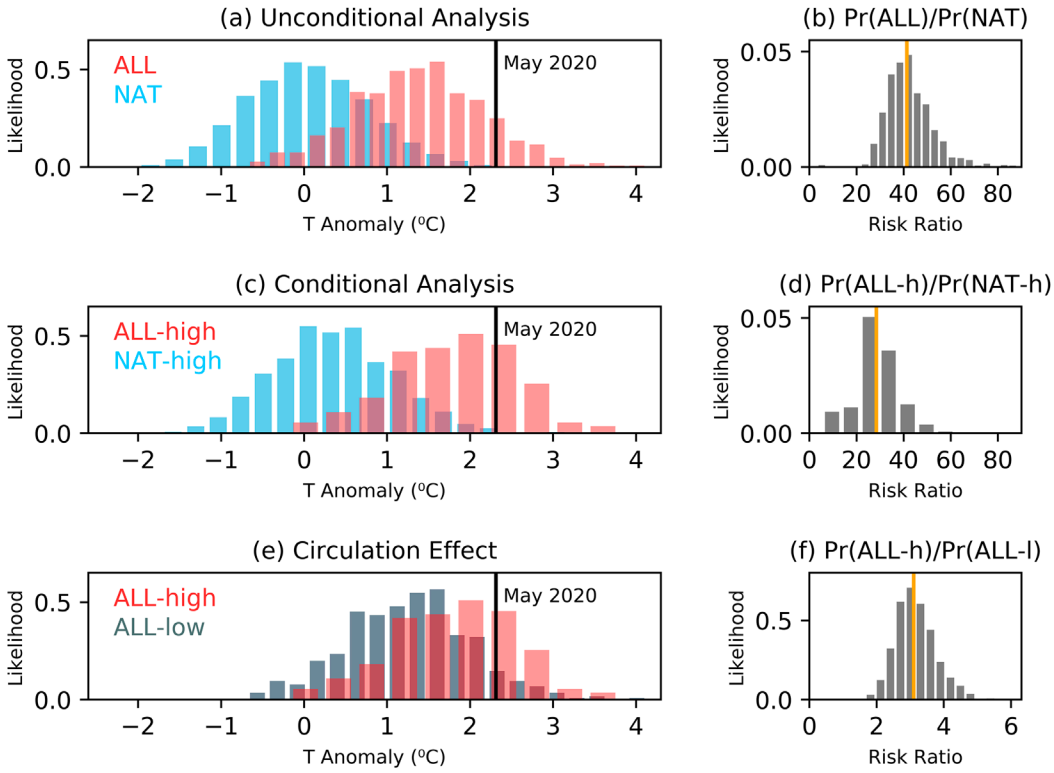

Fig. 2. (a) Normalized distributions of the May mean temperature anomaly with (pink) and without (blue) human influence from the unconditional analysis. The vertical black line marks the May 2020 anomaly. (b) Risk ratio showing the increase in probability due to human influence. The vertical orange line marks the best estimate (50th percentile). (c),(d) As in (a),(b), but for the conditional analysis with probabilities estimated for months with a similar circulation to May 2020. (e) Normalized distributions of the May mean temperature in the present-day climate for seasons with high (pink) and low (gray) correlations to the May 2020 circulation pattern. (f) Risk ratio showing the increase in probability due to the atmospheric circulation effect.

Table 1. Attribution results. Best estimates of the return time, the risk ratio, and their associated 5%–95% uncertainty range (in brackets). Results shown for the unconditional analysis, the analysis conditioned on the circulation pattern and for the assessment of the circulation effect. Return times are shown with (ALL) and without (NAT) the effect of human influence. Conditional estimates use modeled months with high (>0.6) and low (<0.6) correlations with the 2020 circulation pattern.

	Return time (yr)	Return time (yr)	Risk ratio
Unconditional attr.	ALL	NAT	Pr(ALL)/Pr(NAT)
(General case)	8.90 (7.65–10.78)	367 (281–527)	41.27 (29.47–60.36)
Conditional analysis	ALL-high	NAT-high	Pr(ALL-h)/Pr(NAT-h)
(2020-like circulation)	4.15 (3.45–5.29)	119 (35.23–180)	28.37 (8.72–44.42)
Circulation effect	ALL-high	ALL-low	Pr(ALL-h)/Pr(ALL-low)
	4.15 (3.45–5.29)	12.94 (10.43–16.57)	3.10 (2.29–4.28)

about 15 years, while the NAT probability is less affected and changes from 367 to 393. The risk ratio is thus reduced from 41 to 26. Despite these differences, we conclude there is a broadly consistent indication of the estimated anthropogenic impact in terms of its order of magnitude but acknowledge the uncertainty in our results linked to the ensemble construction.

We also conduct an independent assessment with HadCRUT4 observations using the approach of Christidis and Stott (2021). We first remove the smoothed forced change from the observational time series, based on the ALL ensemble mean (white line in Fig. 1c). The remaining anomalies in years 1900–2020 provide the NAT probability. We then add back the forced response corresponding to year 2020, estimated again from the ALL ensemble mean, and compute the ALL probability. The ALL probabilities from HadCRUT4 are in good agreement with CMIP6 (return time: 9 years, uncertainty range: 6–15 years). The smaller NAT probabilities have large uncertainties as they cannot be adequately estimated with the smaller observational sample. Nevertheless, the lower bound of the NAT return time is also of the order of a few hundred years, similar to what the models suggest.

Conditional attribution.

We next derive ALL and NAT probabilities for the extreme event under anticyclonic conditions similar to those in May 2020. As in previous work (Christidis et al. 2018), we sub-sample the model anomalies by selecting months that have similar or different circulation patterns to May 2020 over the reference region, as determined by correlation coefficients above or below 0.6. We confirm that estimating correlations over wider areas would not considerably change our attribution results. Pattern correlations between the reanalysis Z500 anomalies in May over western Europe (Fig. 1b) and simulated May anomalies are thus computed. We then use the high-correlation samples (ALL-high and NAT-high) to infer conditional probabilities (Table 1). We find again that human influence clearly shifts the distribution to warmer temperatures (Fig. 2b), making the 2020 event about 30 times more likely to occur (Fig. 2c, Table 1). As expected, the return times of warm extremes are lower in the conditional case compared to the general case, since the presence of anticyclonic conditions favors warm anomalies. However, the estimated risk ratio is of the same order as in the general case. We finally assess how much more likely the event becomes in the present-day climate under persistent anticyclonic conditions compared to other circulation states. We do this by comparing the ALL-high and ALL-low probabilities (Figs. 2d,e, Table 1) and estimate that May months at least as warm as 2020 become 2–4 times more likely.

Discussion.

Using a suite of 11 state-of-the-art climate models we show that the unprecedented May temperature of 2020 in western Europe is becoming increasingly common under the influence of anthropogenic forcings. There are of course uncertainties in model-based assessments (e.g., biases, model limitations, future emission scenarios), but the level of agreement with simpler approximate probability estimates from observations is reassuring. The models suggest that the return time of May heatwaves with temperatures at least as high as in 2020 has been reduced from centuries to under a decade, although the precise estimated change is sensitive to the ensemble used, as already discussed. While spring heatwaves may generally be expected to have less adverse impacts than summer heatwaves, continuous warming in western Europe means that May would gradually bear a closer resemblance to summer months with possibly serious socio-economic repercussions (e.g., increased heat stress and mortality spikes, strain on energy and water availability, increased wildfire risk, agricultural losses, etc.). Therefore, attribution studies like ours provide valuable information to help communities reduce their vulnerability to anthropogenic climate change.

Acknowledgments. This work was supported by the Met Office Hadley Centre Climate Programme funded by BEIS and Defra.

References

Bindoff, N. L., and Coauthors, 2013: Detection and attribution of climate change: From global to regional. *Climate Change 2013: The Physical Science Basis.* T. F. Stocker et al., Eds., Cambridge University Press, 867–952.

Christidis, N., and P. A. Stott, 2021: Extremely warm days in the UK in winter 2018/19 [in "Explaining Extremes of 2019 from a Climate Perspective"]. *Bull. Amer. Meteor. Soc.,* **102** (1), S39–S44, https://doi.org/10.1175/BAMS-D-20-0123.1.

——, ——, S. Brown, D. J. Karoly, and J. Caesar, 2007: Human contribution to the lengthening of the growing season during 1950–1999. *J. Climate,* **20,** 5441–5454, https://doi.org/10.1175/2007JCLI1568.1.

——, ——, A. Scaife, A. Arribas, G. S. Jones, D. Copsey, J. R. Knight, and W. J. Tennant, 2013: A new HadGEM3-A based system for attribution of weather and climate-related extreme events. *J. Climate,* **26,** 2756–2783, https://doi.org/10.1175/JCLI-D-12-00169.1.

——, A. Ciavarella, and P. A. Stott, 2018: Different ways of framing event attribution questions: The example of warm and wet winters in the UK similar to 2015/16. *J. Climate,* **31,** 4827–4845, https://doi.org/10.1175/JCLI-D-17-0464.1.

——, M. McCarthy, and P. A. Stott, 2021: The increasing likelihood of temperatures above 30 to 40°C in the United Kingdom. *Nat. Commun.,* **11,** 3093, https://doi.org/10.1038/s41467-020-16834-0.

Ciavarella, A., and Coauthors, 2021: Prolonged Siberian heat of 2020 almost impossible without human influence. *Climatic Change,* **166,** 9, https://doi.org/10.1007/s10584-021-03052-w.

Di Liberto, T., 2020: May 2020: Global temperatures tie for record hottest. *ClimateWatch Magazine,* 15 June 2020, https://www.climate.gov/news-features/understanding-climate/may-2020-global-temperatures-tie-record-hottest.

Eyring, V., S. Bony, G. A. Meehl, C. A. Senior, B. Stevens, R. J. Stouffer, and K. E. Taylor, 2016: Overview of the Coupled Model Intercomparison Project Phase 6 (CMIP6) experimental design and organization. *Geosci. Model Dev.,* **9,** 1937–1958, https://doi.org/10.5194/gmd-9-1937-2016.

Kalnay, E., and Coauthors, 1996: The NCEP/NCAR 40-Year Reanalysis Project. *Bull. Amer. Meteor. Soc.,* **77,** 437–471, https://doi.org/10.1175/1520-0477(1996)077<0437:TNYRP>2.0.CO;2.

Morice, C. P., J. J. Kennedy, N. A. Rayner, and P. D. Jones, 2012: Quantifying uncertainties in global and regional temperature change using an ensemble of observational estimates: The HadCRUT4 dataset. *J. Geophys. Res.,* **117,** D08101, https://doi.org/10.1029/2011JD017187.

Riahi, K., and Coauthors, 2017: The Shared Socioeconomic Pathways and their energy, land use, and greenhouse gas emissions implications: An overview. *Global Environ. Change,* **42,** 153–168, https://doi.org/10.1016/j.gloenvcha.2016.05.009.

Ruosteenoja, K., J. Räisänen, A. Venäläinen, and M. Kämäräinen, 2015: Projections for the duration and degree days of the thermal growing season in Europe derived from CMIP5 model output. *Int. J. Climatol.,* **36,** 3039–3055, https://doi.org/10.1002/joc.4535.

Stott, P. A., and Coauthors, 2016: Attribution of extreme weather and climate-related events. *Wiley Interdiscip. Rev.: Climate Change,* **7,** 23–41, https://doi.org/10.1002/wcc.380.